Journal of Ceramic Processing Research. Vol. 11, No. 1, pp. 69~73 (2010)

J O U R N A L O F
Ceramic Processing Research

Pulsed current activated combustion synthesis and consolidation of nanostructured $TaSi_2$

In-Yong Ko[a], Jeong-Hwan Park[a,b], Kee-Seok Nam[c] and In-Jin Shon[a, b]*

[a]*Division of Advanced Materials Engineering, the Research Center of Advanced Materials Development, Chonbuk National University, 664-14 Deokjin-dong 1-ga, Deokjin-gu, Jeonju, Jeonbuk 561-756, Republic of Korea*

[b]*Department of Hydrogen and Fuel Cells Engineering, Specialized Graduate School, Chonbuk National University, 664-14 Deokjin-dong 1-ga, Deokjin-gu, Jeonju, Jeonbuk 561-756, Republic of Korea*

[c]*Korea Institute of Materials Science 531 Changwondaero, Changwon, Gyeongnam, 641-831, Korea*

Dense nanostructured $TaSi_2$ was synthesized by a pulsed current activated combustion synthesis (PCACS) method within 2 minunites in a one step from mechanically activated powders of Ta and Si. Simultaneous combustion synthesis and densification were accomplished under the combined effects of a pulsed current and mechanical pressure. Highly dense $TaSi_2$ with a relative density of up to 98% theoretical was produced under simultaneous application of a 60 MPa pressure and the pulsed current. The average grain size and mechanical properties (hardness and fracture toughness) of the compound were investigated.

Key words: Pulsed current activated combustion, Intermetallic, Nanophase, $TaSi_2$.

Introduction

Interest in refractory metal silicides has increased significantly in recent years because of their potential application as high-temperature structural materials [1]. This class of materials has an attractive combination of properties, including high melting temperature, high modulus, high oxidation resistance in air, and a relatively low density [2, 3]. Furthermore, the disilicides, in particular $TaSi_2$, $TiSi_2$, $MoSi_2$, $NbSi_2$, and WSi_2, have been used as Schottky barriers, ohmic contacts, gate materials, and interconnectors in intergrated circuits, as a result of their low electrical resistivity, high stability, and good compatibility with silicon substrates [4, 5].

Nanostructured materials have been widely investigated because they display a wide functional diversity and exhibit enhanced or different properties compared with bulk materials [6]. In particular, in the case of nanostructured ceramics, the presence of a large fraction of grain boundaries can lead to unusual or better mechanical, electrical, optical, sensing, magnetic, and biomedical properties [7-12]. Recently, nanocrystalline powders have been developed by co-pricipitation, a thermochemical and thermomechanical process named the spray conversion process (SCP) and high energy milling [13, 14]. However, the grain size in sintered materials becomes much larger than that in pre-sintered powders due to the fast grain growth during a conventional sintering process. Therefore, even though the initial particle size is less than 100 nm, the grain size increases rapidly up to 500 nm or larger during the conventional sintering [15]. So, controlling grain growth during sintering is one of the keys to the commercial success of nanostructured materials. In this regard, the pulsed current activated combustion sintering (PCACS) method which can make dense materials within 2 minuites, has been shown to be effective in achieving this goal [16-21].

The objective of this study is to investigate the preparation of dense nanophase $TaSi_2$ by the PCACS method starting from a mixture of mechanically activated Ta and Si powders. The interaction between these phases, i.e :

$$Ta + 2Si \rightarrow TaSi_2 \quad (1)$$

is thermodynamically feasible, as can be seen from Fig. 1.

Experimental Procedure

Powders of 99.97% pure tantalum (–325 mesh, Alfa Products, Ward Hill, MA) and 99% pure silicon (–325 mesh, Aldrich Products, Milwaukee, WI) were used as starting materials. Fig. 2 shows the SEM images of the raw materials used. Powder mixtures of Ta and Si in the molar proportion of 1 : 2 were first milled in a high-energy ball mill (Pulverisette-5, planetary mill) at 250 rpm for 10 h. Tungsten carbide balls (5 mm in diameter) were used in a sealed cylindrical stainless steel vial under an argon atmosphere. The weight ratio of ball-to-powder was 30 : 1. Milling resulted in a significant reduction of

*Corresponding author:
Tel : +82 63 270 2381
Fax: +82 63 270 2386
E-mail: ijshon@chonbuk.ac.kr

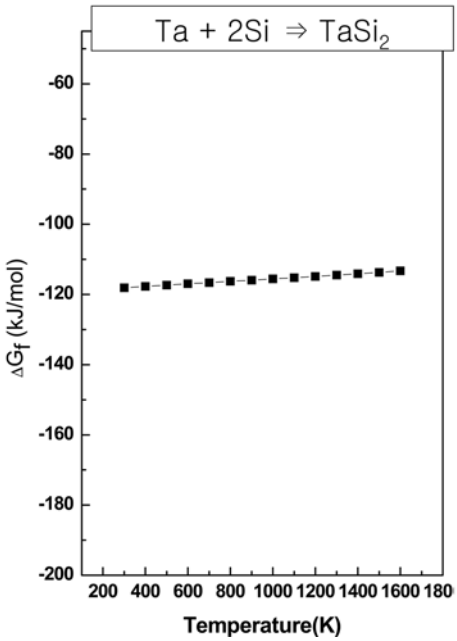

Fig. 1. Temperature dependence of the Gibbs free energy variation by interaction of tantalum with silicon.

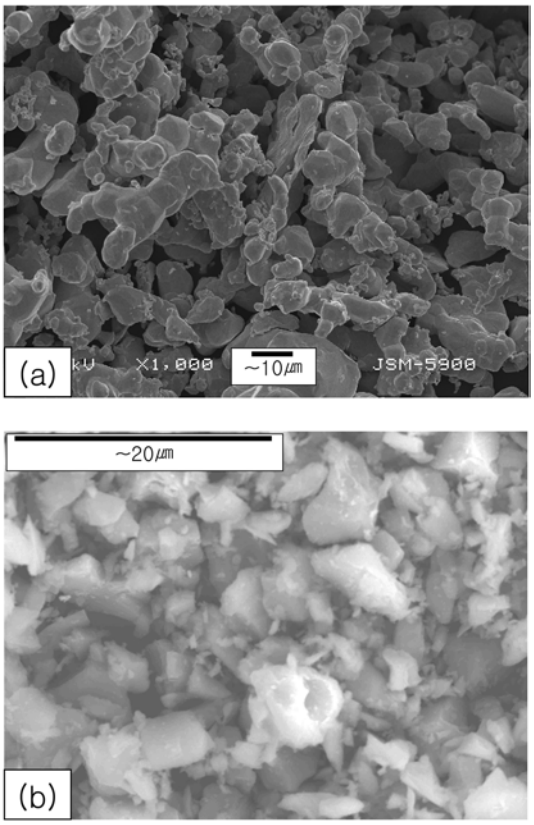

Fig. 2. Scanning electron microscope images of raw materials : (a) tantalum (b) silicon powder.

grain size. The grain size and the internal strain were calculated by Suryanarayana and Norton's formula [22]:

$$B_r(B_{crystalline} + B_{strain})\cos\theta = k\lambda/L + \eta\sin\theta \quad (2)$$

where B_r is the full width at half-maximum (FWHM) of

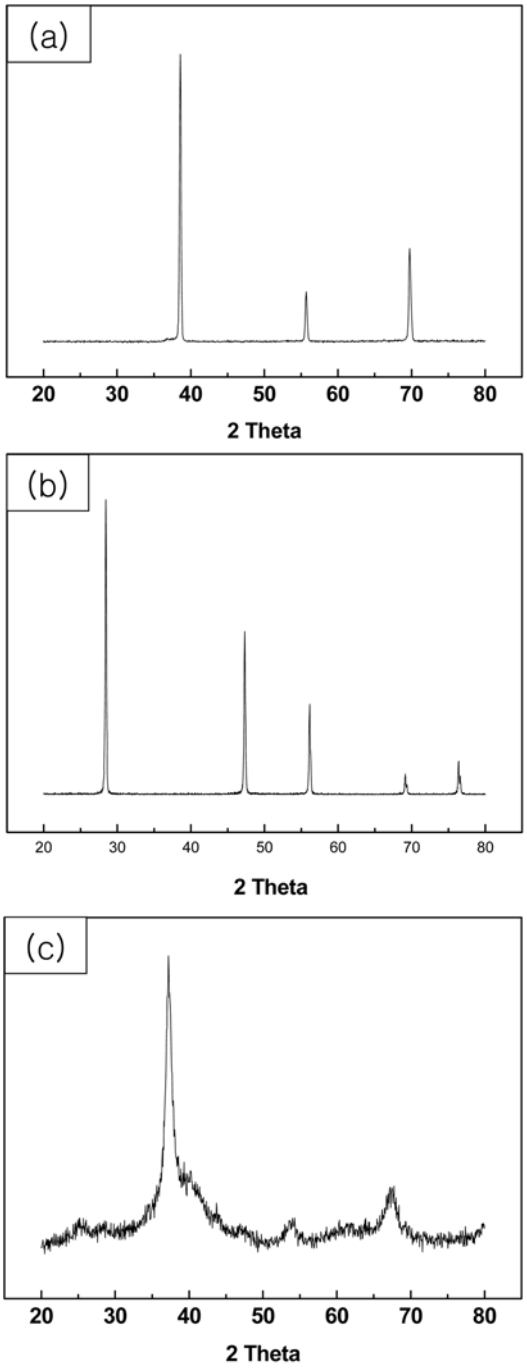

Fig. 3. XRD patterns of raw materials : (a) Ta, (b) Si and (c) milled Ta+2Si.

the diffraction peak after instrumental correction; $B_{crystalline}$ and B_{strain} are the FWHM caused by small grain size and internal strain, respectively; k is a constant (with a value of 0.9); λ is the wavelength of the X-ray radiation; L and η are the grain size and internal strain, respectively; and θ is the Bragg angle. The parameters B and B_r follow Cauchy's form with the relationship: $B = B_r + B_s$, where B and B_s are FWHM of the broadened Bragg peaks and a standard sample's Bragg peaks, respectively. Fig. 3 shows XRD patterns of the raw powders and the milled Ta + 2Si powder mixture. The FWHM of the milled powder is

greater than that of the raw powders due to internal strain and grain size reduction. The average grain size of the milled Ta powders was determined as 39 nm.

After milling, the mixed powders were placed in a graphite die (outside diameter, 45 mm; inside diameter, 20 mm; height, 40 mm) and then introduced into the pulsed current activated combustion sythesis system made by Eltek Co. in the Republic of Korea. Schematic a diagram of this method is shown in Fig. 4. The system was first evacuated and a uniaxial pressure of 60 MPa was applied. The PCACS apparatus includes an 18 V, 2800 A DC power supply (which provides a pulsed current with 20 ms on time and 10 ms off time through the sample and die) and a 50 kN uniaxial press. A DC pulsed current was then activated and maintained until the densification rate was negligible, as indicating by the observed shrinkage of the sample. Sample shrinkage is measured in real time by a linear gauge measuring the vertical displacement. Temperatures were measured by a pyrometer focused on the surface of the graphite die. The heating rates were approximately 900 K·minutes^{-1} in the process. At the end of the process, the pulsed current was turned off and the sample was allowed to cool to room temperature. The entire process of densification using the PCACS technique consists of four major control stages. These are chamber evacuation, pressure application, power application, and cool down. The process was carried out under a vacuum of 40 mTorr (5.33 Pa).

The relative densities of the synthesized samples were measured by the Archimedes method. Microstructural characterization was made on product samples which had been polished and etched using a solution of HF (10 vol.%), HNO_3 (20 vol.%) and H_2O (70 vol.%) for 90 s at room temperature. Compositional and microstructural analyses of the products were made through X-ray diffraction (XRD) and scanning electron microscopy (SEM) with energy dispersive X-ray analysis (EDAX).

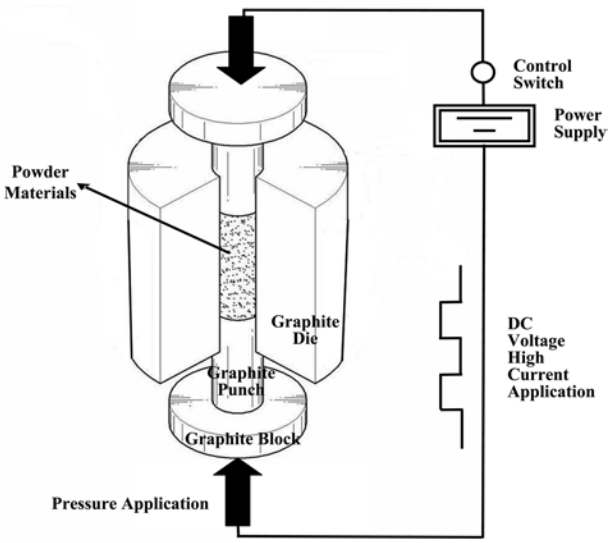

Fig. 4. Schematic diagram of the pulsed current activated combustion synthesis apparatus.

Vickers hardness was measured by performing indentations at a load of 5 kg with a dwell time of 15 s.

Results and Discussion

The variations in shrinkage displacement and temperature with heating time during the processing of the Ta +2Si system are shown Fig. 5. As the pulsed current was applied the shrinkage displacement is initially constant and then abruptly increased at the low temperature of 550 °C. When the reactant mixture of Ta +2Si was heated under 60 MPa pressure to b point, no reaction took place and no significant shrinkage displacement as judged by subsequent XRD and SEM analyses. Fig. 6(a), (b), and (c) show the SEM (secondary electron) images of (a) the powder after milling, (b) the sample heated to b point and (c) the sample heated to 950 °C, respectively. Fig. 6(a) and (b) show the presence of the reactants as separate phases. X-ray diffraction results, shown in Fig. 7(a) and Fig. 7(b) exhibit only peaks pertaining to the reactants Ta and Si. However, when the temperature was raised to 950 °C, the starting powders reacted producing highly dense products. A SEM image of an etched surface of the samples heated to 950 °C under a pressure of 60 MPa is shown in Fig. 6(c). A complete reaction between Ta and Si took place under these conditions. X-ray diffraction analyses of this sample showed peaks of only $TaSi_2$ as indicated in Fig. 7(c). The abrupt increase in the shrinkage displacement at the ignition temperature is due to the increase in density as a result of the molar volume change associated with the formation of $TaSi_2$ from the reactants (Ta and 2Si) and the consolidation of the product. Fig. 8 shows plot of $B_r \sin\theta$ versus $\cos\theta$, indicating that the intercept ($K\lambda/L$) can be used to calculate the crystallite size(L). The average grain size of the sintered $TaSi_2$ calculated by the Suryanarayana and Norton's formula [22] was about 85 nm.

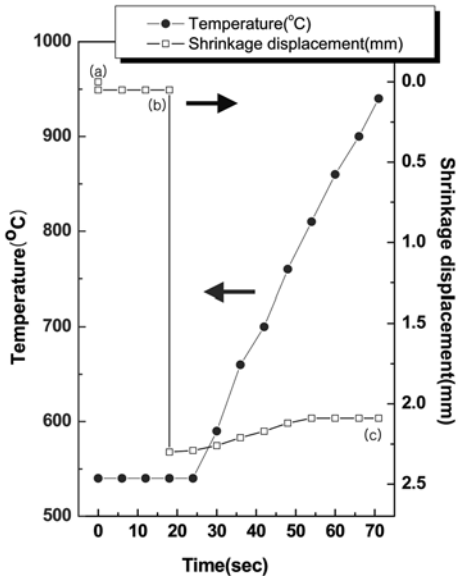

Fig. 5. Variations of temperature and shrinkage displacement with heating time during pulsed current activated combustion synthesis and densification of $TaSi_2$ (under 60 MPa, 2800 A).

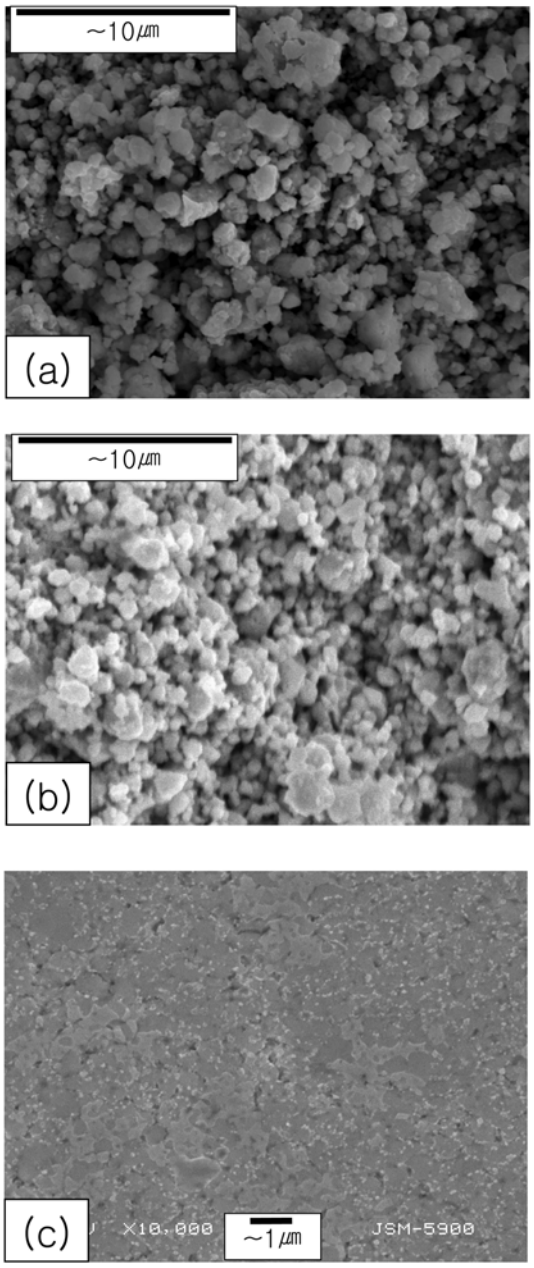

Fig. 6. Scanning electron microscope images of Ta +2Si system : (a) after milling, (b) before combustion synthesis and (c) after combustion synthesis.

Vickers hardness measurements were made on polished sections of the $TaSi_2$ using a 5 kg load with a 15 s dwell time. The calculated hardness value, based on an average of five measurements, of the $TaSi_2$ was 908 kg/mm^2. Indentations with large enough loads produced median cracks around the indent. The length of these cracks permits an estimation of the fracture toughness of the materials by two expressions. The first expression, proposed by Antis *et al*. [23], is :

$$K_{IC} = 0.016(E/H)^{1/2}P/C^{3/2} \quad (3)$$

where E is Young's modulus, H the indentation hardness, P the indentation load, and C the trace length of the crack

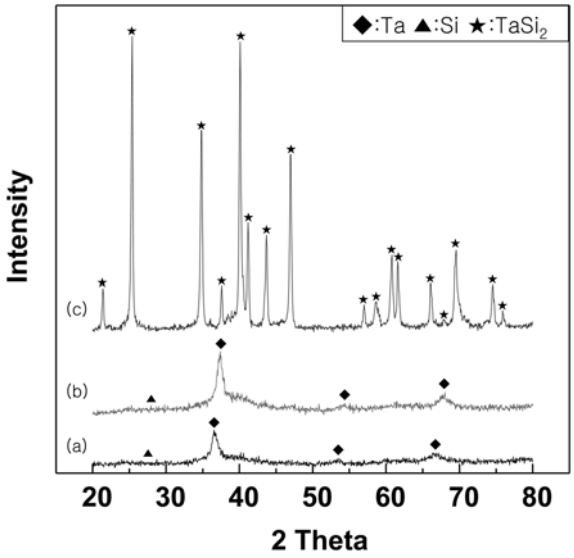

Fig. 7. XRD patterns of the Ta +2Si system : (a) after milling, (b) before combustion synthesis, (c) after combustion synthesis.

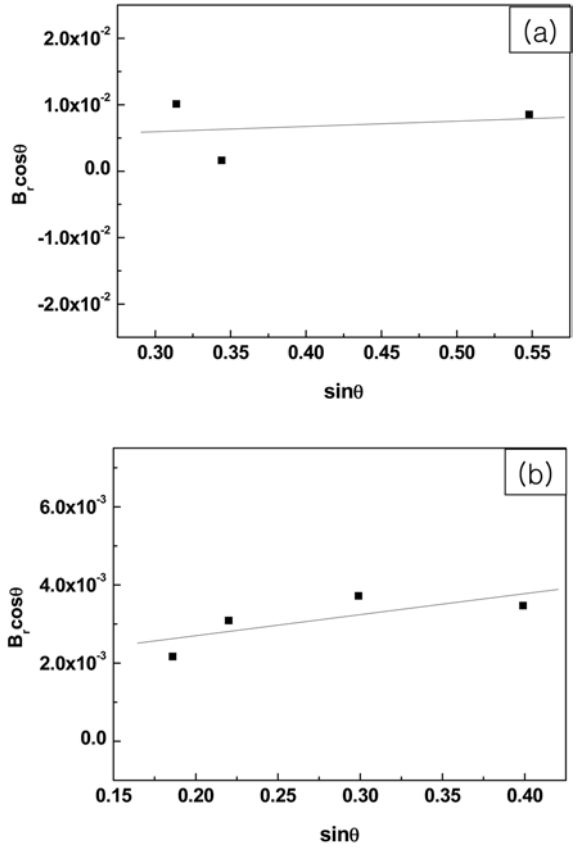

Fig. 8. Plot of $B_r \cos$ against sin, (a) after milling, and (b) after consolidation of $TaSi_2$.

measured from the center of the indentation. The modulus of $TaSi_2$ is 357 GPa [24]. The calculated fracture toughness value of $TaSi_2$ was about 3.5 MPa·m$^{1/2}$. The second expression, proposed by Oh *et al*. and Niihara *et al*. [25, 26], is :

$$K_{IC} = 0.204(c/a)^{-3/2}\cdot H_v \cdot a^{1/2} \quad (4)$$

where c is the trace length of the crack measured from the center of the indentation, a is the half of the average length of two indent diagonals, and H_v is the hardness. The calculated fracture toughness value of $TaSi_2$ using this expression was about 3.7 MPa·$m^{1/2}$. A typical indentation pattern for the $TaSi_2$ is shown in Fig. 9(a). Typically, one to three additional cracks were observed to propagate from the indentation corner. A Higher magnification view of the indentation median crack in the composite is shown in Fig. 9(b). This shows the crack propagates nearly linearly. The absence of reported values for hardness and toughness of $TaSi_2$ precludes making a direct comparison to the results obtained in this study to show the influence of grain size.

Summary

Using the pulsed current activated combustion method, the simultaneous synthesis and densification of nanostructured $TaSi_2$ was accomplished using powders of Ta and Si. Complete synthesis and densification could be achieved in one step within 2 min. The relative density of the composite was 98% under an applied pressure of 60 MPa and the pulsed current. The average grain sizes of the $TaSi_2$ phase was about 85 nm. The average hardness and fracture toughness values obtained were 908 kg/mm^2 and 3.7 MPa·$m^{1/2}$, respectively.

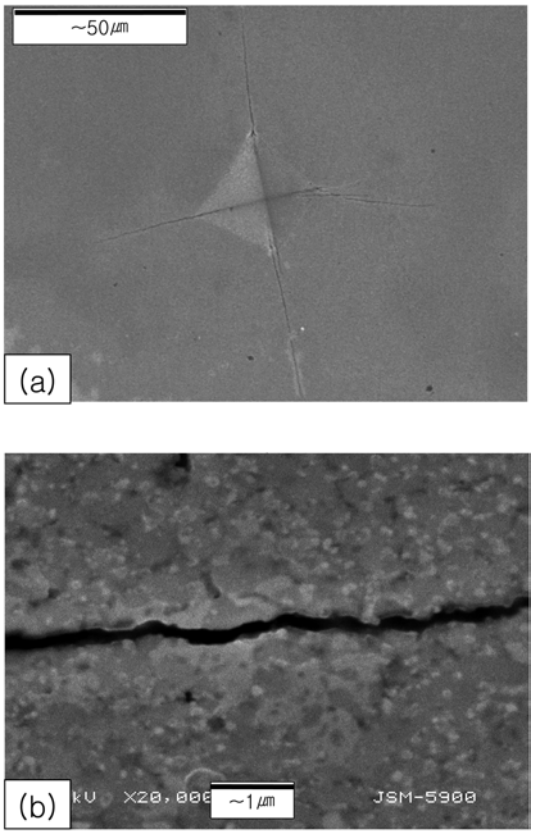

Fig. 9. (a) Vickers hardness indentation and (b) median crack propagating in $TaSi_2$.

Acknowledgements

"This work was supported by the Korea Research Foundation Grant funded by the Korean Government (MOEHRD)" (KRF-2009-0065776).

References

1. N.S. Stoloff, Mater. Sci. Eng. A 261 (1999) 169-180.
2. A.K. Vasudevan and J.J. Petrovic, Mater. Sci. Eng. A 155 (1992) 259-266.
3. G.J. Fan, M.X. Quan, Z.Q. Hu, J. Eckert and L. Schulz, Scripta Mater. 41 (1999) 1147-1151.
4. M.E. Schlesinger, Chem Rev 90 (1990) 607-628.
5. A.K. Vasudevan and J.J. Petrovic, Mater Sci Eng. A 155 (1992) 1-17.
6. H. Gleiter, Mater. 6 (1995) 3-14.
7. J. Karch, R. Birringer and H. Gleiter, Nature 330 (1987) 556-558.
8. A.M. George, J. Iniguez and L. Bellaiche, Nature 413 (2001) 54-57.
9. D. Hreniak and W. Strek, J. Alloys compd. 341 (2002) 183-186.
10. C. Xu, J. Tamaki, N. Miura and N. Yamazoe, Sens. Actuators B 3 (1991) 147-155.
11. D.G. Lamas, A. Caneiro, D. Niebieskikwiat, R.D. Sanchez, D. Garcia, B. Alascio and J. Magn. Mater. 241 (2002) 207-213.
12. E.S. Ahn, N.J. Gleason, A. Nakahira and J.Y. Ying, Nano Lett. 1 (2001) 149-153.
13. Z. Fang and J.W. Eason. Int. J. of Refractory Met. & Hard Mater. 13 (1995) 297-303.
14. A.I.Y. Tok, l.h. Luo, F.Y.C. Boey, Mater. Sci. Eng. A 383 (2004) 229-234.
15. M. Sommer, W.D. Schubert, E. Zobetz and P. Warbichler, Int. J. of Refractory Met. & Hard Mater. 20 (2002) 41-50.
16. Z.A. Munir, I.J. Shon and K. Yamazaki, U. S. Patent No. 5,794,113 (1998).
17. I.J. Shon, Z.A. Munir, K. Yamazaki and K. Shoda, J. Am. Ceram. Soc. 79 (1996) 1875-1880.
18. I.J. Shon, H.C. Kim, D.H. Rho and Z.A. Munir, Mater. Sci. Eng. A 269 (1999) 129-135.
19. I.J. Shon, D.H. Rho, H.C. Kim, Z.A. Munir and J. Alloys compd. 322 (2001) 120-126.
20. I.J. Shon, D.H. Rho and H.C. Kim, Met. & Mater. International 6 (2000) 533-541.
21. C.D. Park, H.C. Kim, I.J. Shon and Z.A. Munir, J. Am. Ceram. Soc. 85 (2002) 2670-2677.
22. C. Suryanarayana and M.G. Norton, X-ray Diffraction A Practical Approach, Plenum Press, New York, 1998.
23. G.R. Anstis, P. Chantikul, B.R. Lawn and D.B. Marshall, J. Am. Ceram. Soc. 64 (1981) 533-538.
24. F. Chu, M. Lei, S.A. Maloy, J.J. Petrovic and T.E. Mitchell, Acta mater. 44 (1996) 3035-3048.
25. D.Y. Oh, H.C. Kim, J.K. Yoon and I.J. Shon, J. Alloys compd. 395 (2005) 174-180.
26. K. Niihara, R. Morena and D.P.H. Hasselman, J. Mater. Sci. Lett. 1 (1982) 12-16.